Interaction of Bovine Serum Albumin with Dipolar Molecules: Fluorescence and Molecular Docking Studies

Bhaswati Bhattacharya, Srinivas Nakka, Lalitha Guruprasad, and Anunay Samanta*

School of Chemistry, University of Hyderabad, Hyderabad 500046, India

Received: September 29, 2008; Revised Manuscript Received: November 22, 2008

Interaction of bovine serum albumin (BSA) with two series of dipolar molecules having both rigid and flexible structures has been studied by monitoring the spectral and temporal behavior of the intramolecular charge transfer fluorescence of the systems. The binding sites of the molecular systems in BSA have been located with the help of docking studies. Three different sites of varying hydrophobicity have been identified where these molecules are located. Binding in the hydrophobic domains of BSA leads to a blue shift of the fluorescence spectra and an enhancement of fluorescence intensity and lifetime. This enhancement is found to be the largest for flexible systems in which internal motion serves as a nonradiative decay route. In the BSA-bound condition, some of the dipolar molecules exhibit not-so-common "dip-rise-dip" time-resolved fluorescence anisotropy profiles. It is shown that a large difference of the fluorescence lifetimes of the protein-bound and unbound molecules is one of the factors that contributes to this kind of anisotropy profiles. As internal motion is often responsible for the short fluorescence lifetime of the flexible dipolar molecules, a large increase in the fluorescence lifetime of these systems occurs if binding to BSA leads to disruption/prevention of this motion. It thus appears that it might be possible to obtain information on the prevention/disruption of nonradiative pathway on protein binding from the anisotropy profiles of the kind discussed above. However, since the present study reveals cases where a large change in fluorescence lifetime also occurs due to other reasons, one needs to be careful prior to making any conclusion.

1. Introduction

Dipolar molecules are routinely used as fluorescence probes for the study of various complex chemical and biological systems.[1−4] Photoexcitation of these molecules, often termed as electron donor−acceptor (EDA) molecules, results in enhanced separation of charge, and these systems commonly emit from an intramolecular charge transfer state. Consequently, the fluorescence parameters of these systems are sensitive to the environment. The wavelength or wavenumber corresponding to the fluorescence maximum, fluorescence quantum yield, nature of the fluorescence decay profile, and fluorescence lifetime are the most commonly monitored fluorescence properties for obtaining information such as the location of the probe in organized assembly, polarity, or viscosity of the microenvironment, etc.[3,4] Time-resolved fluorescence anisotropy is also studied to obtain information on the rotational dynamics of the probes.[5] In homogeneous medium, the fluorescence anisotropy usually decreases exponentially with time, and the associated time constant provides a measure of the rotational dynamics of the molecule. However, when a probe is distributed in two distinct regions of an organized assembly and when the molecular motion in the two regions occurs in significantly different time scales, the time-resolved anisotropy commonly decays biexponentially with the time constants representing two different time scales of the rotation motion in two regions.[5] A complex multiexponential fluorescence anisotropy decay is expected in the case of a more heterogeneous probe distribution. Studies of time-dependence of the anisotropy profiles of molecular systems in various organized assemblies have revealed more complex and somewhat peculiar anisotropy profiles in some cases.[6] During the course of our studies on the fluorescence response of some common fluorescence probes in various organized assemblies, we found some instances where the fluorescence anisotropy profiles are characterized by a rise component. In this manuscript, we report on the interaction of several commonly used fluorescence probes with bovine serum albumin (BSA), whose presence gives rise to complex time-resolved anisotropy profiles of the kind just described for some of the systems.[7]

Probe molecules belonging to two classes, aminocoumarins and aminonitrobenzoxadiazoles, have been chosen for this purpose (Chart 1). Both rigid and flexible aminocoumarins have been selected. Although C153 is perhaps the most extensively used probe for the study of solvation dynamics in different media,[8] other coumarin derivatives are also frequently used as fluorescent probes for studying the interaction with macromolecules such as surfactants[9] and proteins.[10] Twisting (internal rotation) of the amino group is known to play an important role in dictating the fluorescence efficiency and lifetime of aminocoumarins bearing flexible amino groups.[11] A low-lying nonfluorescent twisted intramolecular charge transfer (TICT) state has been speculated in the case of flexible aminocoumarins.[11] The twisting motion of the dialkylamino moiety is severely restricted in environments of cyclodextrins, and micelles.[3b] Literature suggests that constrained environment of protein suppresses the formation of the TICT state in these systems.[10b,12] 4-Amino-7-nitrobenz-oxa-1,3-diazoles (NBD) are also extensively used as EDA fluorophores for the study of biological and model membranes.[13] NBD chloride has often been used for labeling proteins, in exploring the protein structure and conformational changes.[14] Fluorescence sensory behavior of NBD-labeled supramolecular systems toward the transition metal

* Corresponding author e-mail: assc@uohyd.ernet.in.

10.1021/jp808611b CCC: $40.75
Published on Web 01/28/2009

CHART 1: Chemical formula and abbreviation of the probe molecules used in this work

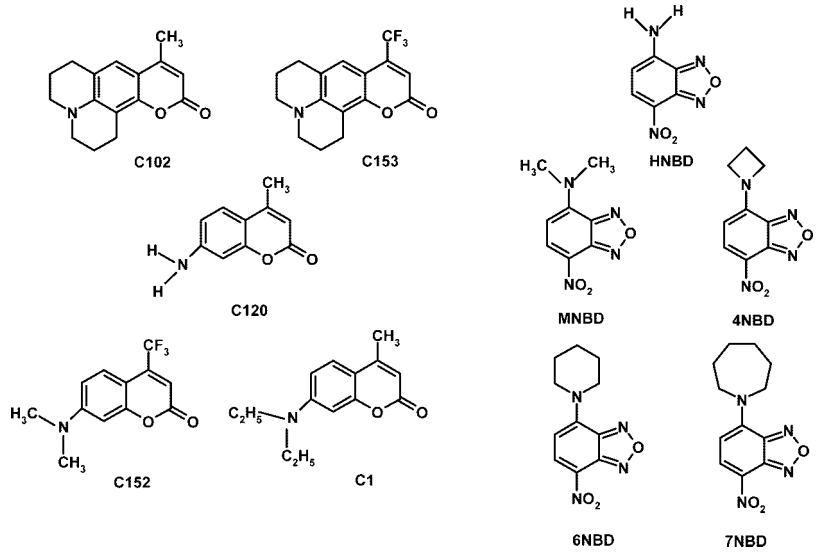

ions has also been studied.[15] Although early studies indicated the involvement of a nonemissive TICT state in the photophysics of NBD derivatives,[16] a more detailed and recent study on several structurally related NBD derivatives has indicated that nonradiative deactivation in these systems is better described by nitrogen inversion than by twisting of the amino functionality.[17] Nevertheless, it is expected that internal rotation or nitrogen inversion will be significantly retarded in the protein-bound condition. The rigid probes that we have selected here are expected to serve as reference systems in which no increase in fluorescence intensity or lifetime is expected due to suppression of the internal motion.

As stated, this work is primarily triggered by our observation of complex time-dependent anisotropy profiles of some commonly used fluorescence probes in the presence of BSA. Our primary objective is not only to understand the nature of the anisotropy profiles, but also to find out whether the nature of anisotropy profile has any connection to the internal rotation in flexible aminocoumarins or nitrogen inversion in the NBD derivatives. If one can indeed establish such a connection, it might be possible to extract information relating to the internal motion in the molecule from the anisotropy profiles, which is something that has not been explored previously. In addition to the steady-state and time-resolved fluorescence behavior of the molecules in the presence of different quantity of BSA, we have also investigated the local environment of the probes in BSA-bound condition through molecular docking studies.

2. Materials and Methods

The coumarin derivatives (laser grade, Exciton), BSA (Sigma), and cetyltrimethylammonium bromide (CTAB, Aldrich) were used as received, whereas 1-butyl-3-methylimidazolium hexafluorophosphate (bmim[PF_6]) was synthesized according to the published procedure.[18] The NBD derivatives were synthesized according to a published procedure.[17] Millipore water was used for solution preparations. BSA and probe solutions were prepared in phosphate buffer (pH 7.0) at room temperature.

The absorption and steady-state fluorescence spectra were recorded on a UV−visible spectrophotometer (Cary100, Varian) and a spectrofluorimeter (FluoroLog-3, Horiba Jobin Yvon), respectively. The fluorescence spectra were corrected for the instrumental response. The concentration of the dipolar molecules was maintained around $(1-3) \times 10^{-5}$ M for fluorescence measurements. A 1 cm path length cuvette was used for all fluorescence studies. Fluorescence quantum yield of HNBD was determined using MNBD as reference ($\phi_f = 0.01$ in water),[17] and the quantum yields of the coumarin and other NBD derivatives were collected from literature.[11b,17,19,20]

Time-resolved fluorescence measurements were carried out using a time-correlated single-photon counting (TCSPC) spectrometer (Horiba Jobin Yvon IBH). Diode lasers ($\lambda_{exc} = 374$ nm for coumarin derivatives and 439 nm for NBD derivatives) were used as the excitation sources, and an MCP photomultiplier (Hamamatsu R3809U-50) was used as the detector (response time 40 ps). The instrument response function of the experimental setup was limited by the fwhm of the exciting laser pulse and was 65 ps for 374 nm excitation and 98 ps for 439 nm excitation. The lamp profile was recorded by placing a scatterer (dilute solution of Ludox in water) in place of the sample. Decay curves were analyzed by nonlinear least-squares iteration procedure using IBH DAS6 (Version 2.2) decay analysis software. The quality of the fits was assessed by the χ^2 values and distribution of residuals. The anisotropy measurements were performed using two polarizers (300−800 nm) by placing one of them in the excitation beam path and the other in front of the detector. IBH software was used for data collection and analysis of the anisotropy data.

The amino acid sequence corresponding to bovine serum albumin was obtained from the Web site http://www.ncbi.nlm.nih.gov/ (NCBI_ID: CAA76847). PDB BLAST (Web site http://www.ncbi.nlm.nih.-gov/BLAST/) with this sequence as query against the protein structure databank identified several structures of human serum albumin. The 3D structure of human serum albumin (PDB ID: 1AO6) was used as template structure for homology modeling, using MODELLER[21] module available in InsightII, Accelrys. The structure was validated using PROCHECK,[22] which measures the stereochemical quality of the protein structure, and Profiles-3D,[23] which measures the compatibility of protein sequence with its model structure.

The structures of the molecular systems were refined using ChemSketch [http://www.acdlabs.com/]. Later, these compounds were docked using AutoDock (3.05) into the 3D structure of BSA. AutoDock[24] uses the Lamarckian genetic algorithm to search for the optimum binding site of small molecules to the protein. To recognize the binding sites in BSA, blind docking was carried out, the grid size set to 100, 100, and 100 along *X*-,

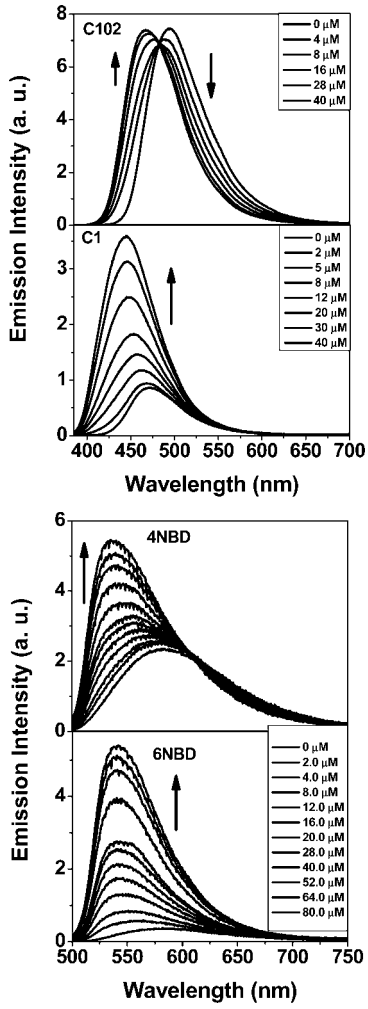

Figure 1. Representative spectra of coumarins and NBD derivatives showing the effect of BSA on the fluorescence behavior.

Y-, and *Z*-axis with 0.603 Å grid spacing. The center of the grid was set to 31.130, 31.715, and 26.672 Å. The AutoDocking parameters used were, GA population size: 150; maximum number of energy evaluations; 250 000. During docking, a maximum number of 10 conformers was considered for each molecule, and the rms (root-mean-square) cluster tolerance was set to 0.5 Å. The conformation with the lowest binding free energy was used for further analysis.

3. Results and Discussion:

3.1. Steady State Behavior. Addition of BSA results in small changes in the absorption spectra of the systems. Interestingly, BSA induced changes in the fluorescence spectra of the systems (spectral shift or intensity distribution) are much more pronounced. This is evident from some of the representative spectra shown in Figure 1.

With the exception of C120, all systems show significant blue shift of the emission maximum in presence of BSA. On the basis of the spectral data of the systems in different solvents, one can attribute this blue shift to the entry of these molecules from aqueous solution to the hydrophobic domains of BSA. Figure 2 shows how the spectral shift of different systems varies with concentration of BSA. Lack of spectral shift for C120 is consistent with its hydrophilic nature.[19] That the spectral shift of most of the other systems is accompanied by enhancement of fluorescence intensity is consistent with a higher fluorescence yield of these systems in a relatively less polar environment.

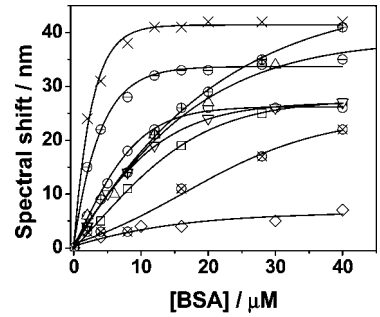

Figure 2. Plot of shift of the spectral maximum for the systems (C102: □; C153: ○; C152: Δ; C1: ▽; HNBD: ◇; MNBD: ⊗; 4NBD: ⊕; 6NBD: ×; 7NBD: ⊖) versus concentration of BSA.

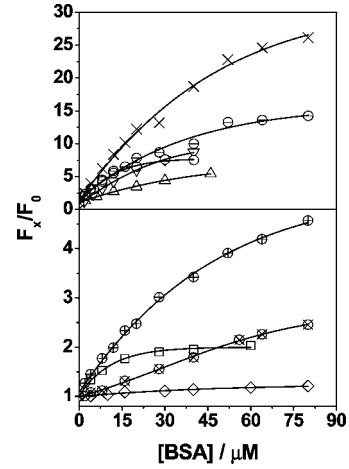

Figure 3. Plot of enhancement of fluorescence intensity (measured at a wavelength where the fluorescence intensity is maximum in presence of BSA) for the systems (C102: □; C153: ○; C152: Δ; C1: ▽; HNBD: ◇; MNBD: ⊗; 4NBD: ⊕; 6NBD: ×; 7NBD: ⊖) versus the concentration of BSA.

TABLE 1: Steady-state Fluorescence Parameters and the Measured Binding Constants for the Systems

system	Φ_f [a]	Blue shift[b] (nm)	FE[c]
C102	0.66	27	1.8
C153	0.12	26	7.5
C120	0.94	nil	0.9
C152	0.06	37	5.4
C1	0.055	27	8.7
HNBD	0.028	7	1.1
MNBD	0.01	22	1.6
4NBD	0.02	41	3.0
6NBD	0.002	42	18.7
7NBD	0.004	35	9.3

[a] For [BSA] = 0, collected from refs 11b, 17, 19, 20. [b] Shift of the fluorescence maximum observed for [BSA] = 40 μM. [c] Measured at the fluorescence maximum for [BSA] = 40 μM.

The extent of fluorescence enhancement (FE) varies from system to system. The variation of fluorescence intensity of the systems as a function of the concentration of BSA is shown in Figure 3. C102, which shows blue shift comparable to other systems (indicating its binding in the hydrophobic pocket of BSA), however displays small FE. This may not be surprising as ϕ_f of C102 is quite high in aqueous environment (Table 1). Very similar is the case of C120 for which no FE, but slight quenching, is observed. Interesting are the cases of 6NBD and 7NBD among the NBD derivatives and C1 and C152 among the coumarins. These systems show higher enhancement compared to the remaining systems of each class. For C1, C152,

6NBD, and 7NBD, a higher FE can be rationalized taking into consideration the fact that FE in these systems not only arises due to binding of these molecular systems in the hydrophobic domain of BSA, but also due to prevention/restriction of internal motion in these systems, which is known to be responsible for low fluorescence efficiency of these systems compared to the remaining ones (Table 1) in polar media.[3b,11,17] It is interesting to note that for 6NBD and 7NBD, the saturation of the spectral shift occurs at a lower concentration of BSA when compared with the saturation of fluorescence intensity. This difference must be related to the fact that although the spectral shift depends only on the polarity of the medium and it saturates as soon as the molecule reaches the most hydrophobic region, the fluorescence intensity of these flexible systems also depends on the constraint provided by the media. A more constrained environment at higher concentrations of BSA can contribute to the observation.

Assuming 1:1 interaction between the two, one can evaluate the binding constants of the probes with BSA by monitoring the changes in the fluorescence intensity using frequently used equation:[25]

$$1/(F_x - F_0) = 1/(F_\infty - F_0) + 1/(F_\infty - F_0)K[\mathrm{L}]$$

where, F_0, F_x, and F_∞ are the fluorescence intensities of the probes in the absence of BSA, at an intermediate BSA concentration, and at a concentration corresponding to complete interaction, respectively, and [L] is the BSA concentration. Although estimates of the binding constants can be made using this method, precise estimation of the K values from the intensity measurements may not be practical (and hence, not attempted) as for some systems FE is solely due to binding in the hydrophobic domain, whereas for some other systems FE is also due to disruption of the internal motion. For rigid coumarins, the K values are estimated to be around 95×10^3 M^{-1}.

3.2. Time-resolved Behavior. Fluorescence lifetimes of the coumarins vary between 0.4 and 5.9 ns in the aqueous solution. The rigid system C102 has the highest lifetime (Table 2). The other rigid system C153 has a lifetime of 1.7 ns. C1 and C152, for which a low-lying nonfluorescent TICT state has been proposed, are characterized by fluorescence lifetime of 0.4 and 0.5 ns. The fluorescent state of the NBD derivatives is much short-lived. In fact, the fluorescent lifetime of 6NBD and 7NBD are found to be comparable to the pulse width (98 ps) of the exciting pulse and hence could not be determined precisely in the absence of BSA. The short fluorescence lifetime is a reflection of efficient nonradiative deactivation associated with the inversion of the amino nitrogen in these systems.[17] On the other hand, HNBD or 4NBD, for which radiationless process is shown to be unimportant,[17] possess a lifetime of 0.9−1.0 ns.

In the presence of BSA no change in fluorescence lifetime of C120 is observed. This observation is consistent with its hydrophilic nature and its location, where it is exposed to water. For C102, no increase of fluorescence lifetime is observed on its binding in the hydrophobic domain of BSA as the lifetime in aqueous solution is quite long. The decay profiles for the remaining systems are double-exponential (Table 2) in the presence of BSA. Typical decay profiles of a given system in the absence and presence of BSA are shown in Figure 4. The biexponential nature of the decay profiles of the systems in presence of BSA can be interpreted as follows. The short component, whose lifetime is similar/comparable to the lifetime of the probe in aqueous solution, is due to the free (unbound) probe, wherein the long component is due to to the protein-bound probe. The change in amplitude of the two components with gradual addition of BSA is in accordance with the increased population of bound molecules. For some of the systems, in addition to the change in amplitude of the two components, slight change in the lifetime of the short component is also observed. This is perhaps a reflection of the change of the

TABLE 2: Time-resolved Fluorescence Parameters of the Systems in Presence of Different Quantities of BSA

system	[BSA]/μM	τ_1 (a_1)/ns	τ_2 (a_2)/ns	τ_2/τ_1
C102	0	5.9		
	4	5.9		
	16	5.8		
	40	5.7		
C153	0	1.7		
	2	1.7 (0.81)	5.1 (0.19)	3.0
	8	1.8 (0.59)	5.1 (0.41)	2.8
	20	1.8 (0.48)	5.3 (0.52)	2.9
	40	1.7 (0.41)	5.2 (0.59)	3.0
C120	0	5.0		
	2	5.0		
	8	4.9		
	28	4.9		
C152	0	0.5		
	6	0.5 (0.93)	4.4 (0.07)	8.8
	12	0.5 (0.85)	4.6 (0.15)	9.2
	20	0.6 (0.7)	4.7 (0.29)	7.8
	30	0.7 (0.62)	4.8 (0.38)	6.8
C1	0	0.4		
	2	0.3 (0.98)	3.6 (0.02)	12.0
	8	0.4 (0.84)	4.0 (0.16)	10.0
	20	0.5 (0.52)	4.1 (0.48)	8.2
	40	0.6 (0.36)	4.1 (0.64)	6.8
HNBD	0	0.9		
	8	0.9 (0.98)	6.5 (0.02)	7.2
	60	1.0 (0.91)	7.5 (0.09)	7.5
	80	1.1 (0.89)	7.7 (0.11)	7.0
MNBD	0	0.2		
	20	0.3 (0.88)	3.4 (0.12)	11.3
	40	0.5 (0.77)	3.4 (0.23)	6.8
	80	0.6 (0.71)	3.8 (0.29)	6.3
4NBD	0	0.989		
	8	1.0 (0.94)	6.4 (0.06)	6.4
	40	1.2 (0.68)	6.2 (0.32)	5.2
	80	1.5 (0.57)	6.9 (0.43)	4.6
6NBD	0			
	2	0.1 (0.96)	3.8 (0.04)	38.0
	8	0.8 (0.75)	5.3 (0.25)	6.6
	16	1.1 (0.7)	5.4 (0.3)	4.9
	40	1.2 (0.66)	5.4 (0.34)	4.5
	80	1.4 (0.62)	6.0 (0.38)	4.3
7NBD	0			
	2	0.2 (0.77)	4.2 (0.23)	21.0
	8	0.5 (0.87)	4.8 (0.48)	9.6
	16	0.7 (0.85)	5.5 (0.15)	7.8
	40	1.1 (0.85)	6.8 (0.15)	6.2
	80	1.0 (0.86)	6.8 (0.14)	6.8

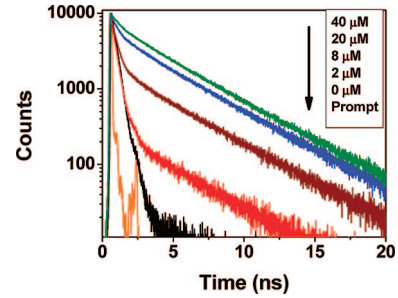

Figure 4. Time-resolved fluorescence profile of C1 monitored at the emission maximum at different concentrations of BSA.

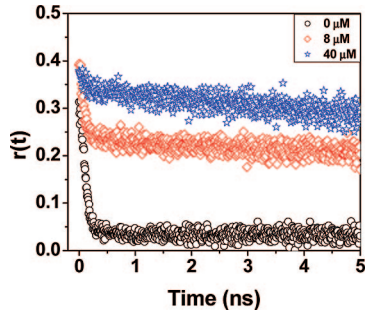

Figure 5. Time-resolved anisotropy profile of C102 for different concentrations of BSA showing biexponential decay.

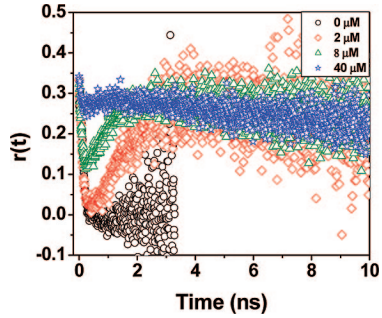

Figure 6. Time-resolved anisotropy profile of C1 for various concentrations of BSA depicting the dip-rise-dip nature of the profile.

microenvironment (e.g., viscosity) around the free molecules with increasing concentration of BSA. It can be seen that the lifetimes of BSA-bound C152, C1, MNBD, 6NBD, and 7NBD are significantly larger than those for the remaining systems. This is a reflection of the restriction of the internal motion in these systems on binding. For the other systems—C153, HNBD, and 4NBD—the increase in fluorescence lifetime on binding to BSA is presumably due to an increase of the radiative transition probability.

Time-resolved fluorescence anisotropy profiles of the systems in the presence of BSA are found to be quite interesting. In the absence of BSA, a single-exponential anisotropy decay with a rotational correlation time of ~110 to 120 ps is observed for most of the systems. This not only suggests that the probe molecules experience a homogeneous environment, but is also consistent with the fact that the sizes of the molecular systems used in this work are comparable. In the presence of BSA, the anisotropy decay is expected to be biexponential because of distinctly different rotational times of the free and protein-bound molecules. This is indeed the case of the rigid system C102 (Figure 5). Even for flexible system such as C1, a similar time-resolved anisotropy profile is observed in other organized assemblies, such as in micelles and room temperature ionic liquids (RTILs).[26] In all these cases, the short anisotropy decay represents the rotational time of the unbound probe molecule, whereas the long component represents the rotational time of the protein-bound probe. Interestingly, for most of the systems, in addition to the decaying short and long anisotropy components, a growth component at intermediate time is also observed (Figure 6) in the presence of BSA, giving "dip-rise-dip" kind of profiles.

This kind of not-so-common time-resolved anisotropy behavior can be explained with the help of a two-component anisotropy equation (eq 1), suggested by Ludescher et. al,[27] and is applicable to one of the simplest of various possible scenarios[6] involving the presence of two distinct species, each characterized by its own lifetime and anisotropy decay.

$$r(t) = r(0)[f_1 \exp(-t/\theta_1) + f_2 \exp(-t/\theta_2)] \quad (1)$$

with

$$f_i(t)=a_i[\exp(-t/\tau_i)]/I(t)$$

where f_i is the time-dependent weighing factor, $I(t)$ is the total intensity decay, and a_i is the amplitude of the intensity decay.

According to eq 1, the nature of the plot of $r(t)$ vs t is governed by initial anisotropy, $r(0)$; rotational times of the free and bound probes, θ_1 and θ_2, respectively; fluorescence lifetimes of the free and bound probes, τ_1 and τ_2, respectively; and the associated amplitudes, a_1 and a_2. It can be shown that if the free and BSA-bound probes are characterized by widely different rotational correlation times, then one obtains anisotropy profiles of the kind shown in Figure 6 when the lifetime and/or amplitudes associated with them are varied (with change of BSA concentration). The curves simulated in Figure 7 using some of the lifetime data presented in Table 2 illustrate this point.

Let us now attempt to understand why some systems such as C1 show the dip-rise-dip anisotropy profile, whereas a rigid probe like C102 does not show a similar behavior. It may be noted that the two rotational times, θ_1 (fast component) and θ_2 (slow component) are very different, as the former is associated with the rotation of the free molecule and the latter represents rotation of the molecule along with a part of the macromolecule. Irrespective of whether a system is rigid or flexible, these quantities are, however, expected to be very similar for all the systems because of their similar size and similar BSA-binding property (except C120). The quantities that are different for various systems are the two lifetime components and amplitudes associated with them. The combined effect of the two is represented by f_1 and f_2. Although earlier studies[6f] have rightly stressed on the importance of the time-dependent weighing factor, $f_i(t)$ in giving rise to the "dip and rise" nature of the anisotropy profile, we find that a dip-rise-dip profile of the kind reported here is best obtained when the two lifetime values are very different. Clearly, the dip-rise-dip anisotropy profile condition is best realized for systems where internal motion is responsible for rapid nonradiative deactivation of the fluorescent state. This is because these systems are characterized by short fluorescence lifetime, and in the protein-bound condition when the internal motion is severly restricted, there occurs a large enhancement of lifetime. Hence, systems such as C1, C152, 6NBD, and 7NBD are more likely to show this kind of anisotropy profiles. Therefore, it may be possible to obtain information on prevention/disruption of internal motion in a flexible molecular system of the kind studied here from the anisotropy profiles. However, since systems like HNBD, for which a large change of fluorescence lifetime occurs on binding to BSA for another reason, it is evident that the internal motion in the system cannot be considered as the sole criterion for generating dip-rise-dip anisotropy profiles; hence, one needs to be careful when interpreting this kind of anisotropy profiles.

3.3. Modeling of Binding Site of BSA. The sequences of BSA and human serum albumin (HSA) share 88% homology.[28,29] The N-terminal 24 amino acid residues in the bovine sequence that did not have an equivalent in the human template crystal structure (PDB code: 1AO6) were not included in the model.

The crystal structure of HSA comprises three domains. The three domains (I, II, III) have similar 3D structures and are highly asymmetric in assembly with 17 disulfide bridges.[30,31] Each domain can be further divided into subdomains "a" and "b", which are composed of six and four α-helices, respectively. A long extended loop traverses the two subdomains to link them

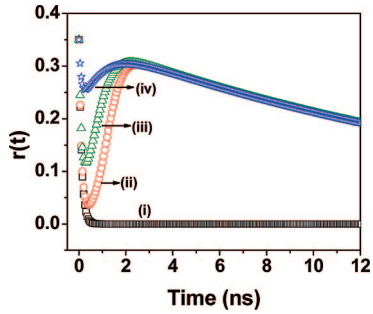

Figure 7. The curves constructed using eq 1 with an initial anisotropy (r_0) of 0.35 and other parameters as follows. Used for (i) $\theta = 0.11$ ns, $\tau = 0.4$ ns; (ii) $\theta_1 = 0.11$ ns, $\theta_2 = 20$ ns, $\tau_1 = 0.3$ ns, $a_1 = 0.975$, $\tau_2 = 3.6$ ns, $a_2 = 0.025$; (iii) $\theta_1 = 0.11$ ns, $\theta_2 = 20$ ns, $\tau_1 = 0.36$ ns, $a_1 = 0.84$, $\tau_2 = 4$ ns, $a_2 = 0.16$; and (iv) $\theta_1 = 0.11$ ns, $\theta_2 = 20$ ns, $\tau_1 = 0.65$ ns, $a_1 = 0.36$, $\tau_2 = 4.1$ ns, $a_2 = 0.64$).

together. The pocket of subdomain IIa corresponds to the drug site I, which is known to be a warfarin binding site, as well as for several other drugs.[32−34] The subdomain IIIa is known to be drug site II, which is similar to drug site I. Thyroxin, octanoate, and some other drugs bind to this site.[35,36] For long-chain fatty acids, three binding sites with entirely different structural environments have been reported.[37] Our model of the BSA shows that the three domains are identical to those in HSA, and the binding sites for the various compounds analyzed in this work have an equivalent binding site in HSA.

The rms deviation corresponding to equivalent C-α atoms in BSA model and HSA structure (PDB code: 1AO6) is 0.303 Å.[38] The analysis of protein structure using Profiles-3D reported a 254/264 score, and the PROCHECK analysis reported that 99.6% amino acid residues are within the allowed regions of the Ramachandran plot.[39]

We have docked 10 systems into the 3D structure of BSA using AutoDock Tools. These models provide the most probable binding sites and poses in the protein that have not resulted in structural alteration of BSA. These molecules occupy three different binding sites in BSA.[40] The molecules in the first binding site are C1, C102, C152, C153, and 7NBD. The molecules in the second binding site are MNBD, 4NBD, and 6NBD. The molecules in the third binding site are HNBD and C120. The location of these sites in the 3D structure of BSA is shown in Scheme 1. It is encouraging to note that the binding sites in bovine are similar to some of the known binding sites in HSA, although no bias was introduced in defining the binding sites in bovine using the AutoDock program.

The first-group molecules are bound at the subdomain IIa, which is known to be drug site I[41−43] (Figure 8). The amino acid residues lining this binding site are comprised of Trp213, His237, Leu241, Tyr149, Arg198, Gln195, Arg194, Ala290, Glu291, and Arg217. These molecules bind to the site essentially via hydrophobic and van Der Waals forces. In some cases, hydrogen bonding interactions have been observed. C1 makes one hydrogen bond with the Arg194 side chain through its carbonyl group. The CH_3 group of C1 makes CH$\cdots\pi$ interactions with the aromatic side chain of Tyr149. The side chain $C^{\beta}H$ of Ala290 makes CH$\cdots\pi$ interactions with the coumarin ring. This coumarin ring also makes $\pi\cdots\pi$ interactions with the guanidinium group of Arg198.

Likewise, C102 and C153 make hydrogen bonding interactions with Arg198 side chain through their carbonyl groups. The CH_3 group of C102 makes makes CH$\cdots\pi$ interactions with the aromatic side chain of Tyr149. The side chain $C^{\beta}H$ of Ala290 makes CH$\cdots\pi$ interactions with the coumarin ring in C102 and C153.

SCHEME 1: Schematic representation of BSA model structure indicating the binding pockets and bound molecules

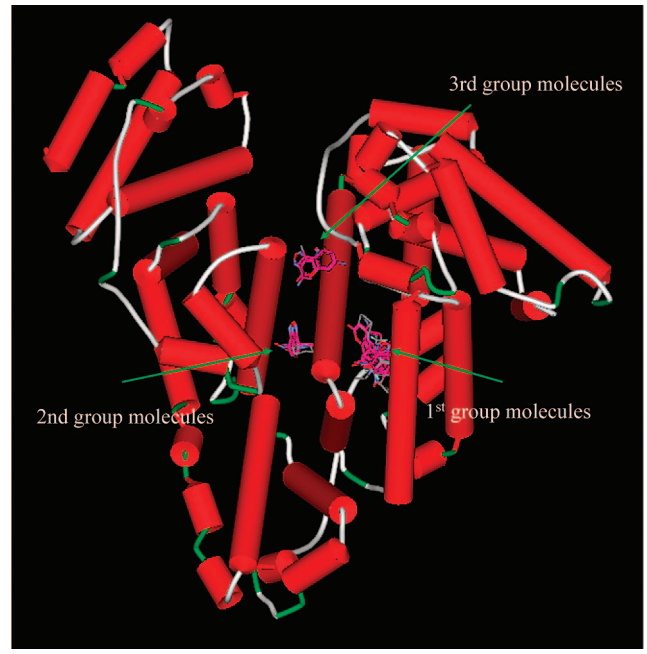

C152 makes four hydrogen bonding interactions with Tyr149 and Arg256 side chains through coumarin ring oxygen and carbonyl oxygen. The side chain $C^{\beta}H$ of Ala290 makes CH$\cdots\pi$ interactions with the coumarin ring of C152. The side chain $C^{\beta}H$ of Ala290 makes CH$\cdots\pi$ interactions with the coumarin ring. The 7-membered cyclic ring in 7NBD makes CH$\cdots\pi$ interactions with the guanidinuim group of Arg198.

These molecules are present within (3.6−3.9) Å distance from Trp213, and the side chains of neighboring hydrophobic residues are located close by. Therefore, it is understandable why these molecular systems display significant blue shift of the fluorescence maxima and how internal rotation in some of the flexible systems is retarded, giving rise to high FE.

The second-group molecules are bound at the interface between subdomains IIa and IIIa (Figure 9). This is located at the bottom of the entrance of the binding pocket of IIa.[40] This binding site, unlike the binding site discussed above, is perhaps selective in the type of compounds that bind. The amino acid residues lining this binding site are comprised of Arg194,

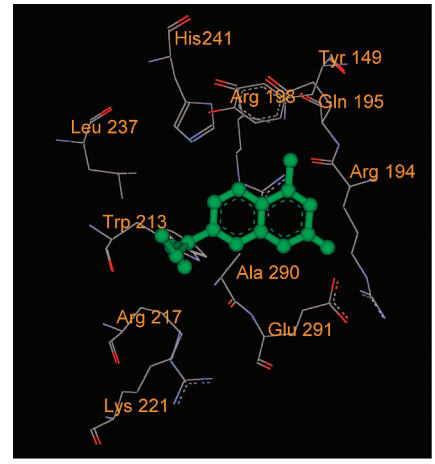

Figure 8. Binding pocket for first group molecules (showing C1) within 4 Å distance.

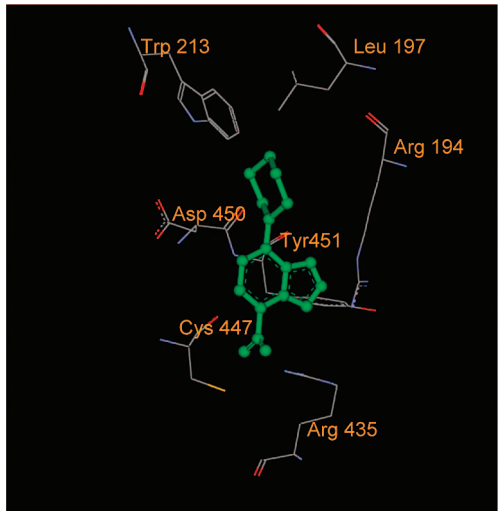

Figure 9. Binding pocket for second-group molecules (showing 6NBD) within 4 Å distance.

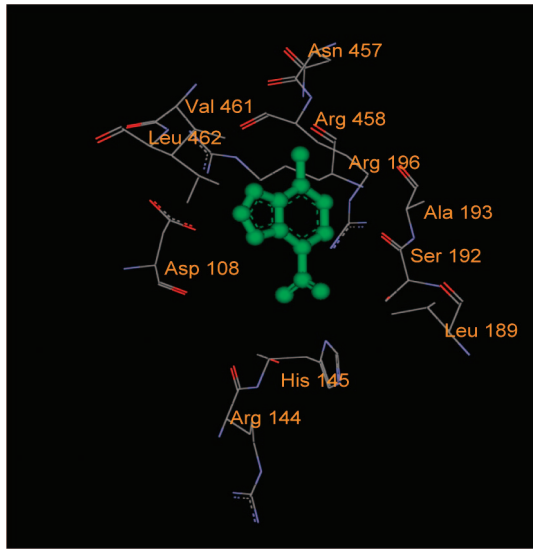

Figure 10. Binding pocket for third group molecules (showing HNBD) within 4 Å distance.

Leu197, Trp213, Arg435, Cys447, Asp450, and Tyr451. The nitro group present in 4NBD, 6NBD, and MNBD make two hydrogen bonding interactions with the Arg435 side chain. In the case of MNBD, $C^{\alpha}H$ of Tyr451 makes CH$\cdots\pi$ interactions with the aromatic ring of MNBD. In this case there is enough room around the methyl groups that allows them to be flexible, hence binding is comparatively weak. The 4-membered cyclic group in 4NBD experiences hydrophobic interactions with the side chains of Leu197 and Leu454. The $C^{\alpha}H$ of Tyr451 makes CH$\cdots\pi$ interactions with the aromatic ring of 4NBD. The 6-membered ring in 6NBD is close to Trp213 (3.6 Å) and to Leu197 (2.8 Å). $C^{\alpha}H$ of Tyr451 makes CH$\cdots\pi$ interactions with the aromatic ring of 6NBD. It is possible that these hydrophobic interactions hold 6NBD in a rigid manner within the binding site, possibly explaining the greater blue shift and FE when bound to protein.

The third-group molecules are bound at the interface between two sub domains IIa and IIIa, which is located just above the entrance of the binding pocket of IIa (Figure 10). The amino acid residues lining this binding site are comprised of Arg196, Arg458, Asp108, His145, Asn457, Val461, Leu462, Ala193, Ser192, Leu189, and Arg144. This site is relatively more exposed to the solvent. The molecules C120 and HNBD are bound to this site. HNBD forms two hydrogen bonding interactions with Arg458 and His145 side chains. The guanidinium group of Arg458 makes $\pi\cdots\pi$ interactions with the aromatic ring of HNBD and C120.

That these compounds prefer a binding site that is highly polar and exposed to the solvent environment explains why HNBD and C120 show less blue shift of the fluorescence maximum compared to the first and second groups of molecules.

Acknowledgment. This work has been supported by the Ramanna Fellowship of the Department of Science and Technology, Government of India, and by the UPE Program of the University Grants Commission. B. B. and S. N. thank the Council of Scientific and Industrial Research for a Fellowship.

Supporting Information Available: This material is available free of charge via the Internet at http://pubs.acs.org.

References and Notes

(1) (a) Michel-Bewryerle, M. E. In *The Reaction Centre of Photosynthetic Bacteria*; Springer Verlag: Berlin, 1995. (b) Wasielewski, M. R. *Chem. Rev.* **1992**, *92*, 435. (c) Gust, D.; Moore, T. A.; Moore, A. L. *Acc. Chem. Res.* **1993**, *26*, 198. (d) Bard, A.; Fox, M. A. *Acc. Chem. Res.* **1995**, *28*, 141. (e) Meyer, T. J. *Acc. Chem. Res.* **1989**, *22*, 163.

(2) (a) Fabrizzi, L.; Poggi, A. *Chem. Soc. Rev.* **1995**, *24*, 197. (b) Shelton, D. B.; Rice, J. E. *Chem. Rev.* **1994**, *94*, 3. (c) Carter, F. L.; Siatoski, R. E.; Woltjen, H. In *Molecular Electronic Devices*; North Holland: Amsterdam, 1988. (d) Barbara, P. F.; Jarzeba, W. *Acc. Chem. Res.* **1988**, *21*, 195.

(3) (a) *Photochemistry in Organised and Constrained Media*; Ramamurthy, V., Eds.; VCH: New York, 1991. (b) Bhattacharyya, K.; Chowdhury, M. *Chem. Rev* **1993**, *93*, 507, and references therein.

(4) (a) *Topics in Fluorescence Spectroscopy*; Lakowicz, J. R., Ed.; Plenum Press: New York, 1994; Vol 4. (b) Kalyanasundram, K. In *Photochemistry in Microheterogeneous Systems*; Academic Press Inc.: London, 1987.

(5) (a) Lakowicz, J. R. In *Principles of Fluorescence Spectroscopy*; 2nd Ed.; Kluwer Academic/Plenum Press: New York, 1999. (b) *Topics in Fluorescence Spectroscopy*; Lakowicz, J. R., Ed.; Plenum Press: New York, 1994; Vol 2.

(6) (a) Jones, B. E.; Beechem, J. M.; Matthews, C. R. *Biochemistry* **1995**, *34*, 1867. (b) Bilsel, O.; Yang, L.; Zitzewitz, J. A.; Beechem, J. M.; Matthews, C. R. *Biochemistry* **1999**, *38*, 4177. (c) Srivastava, A.; Krishnamoorthy, G. *Arch. Biochem. Biophys.* **1997**, *340*, 159. (d) Hudson, B.; Harris, D. L.; Ludescher, R. D.; Ruggiero, A.; Cooney-Freed, A.; Cavalier, S. A. In *Fluorescence in the Biological Sciences*; Taylor, D. L.; Waggoner, A. S.; Lanni, F.; Murphy, R. F.; Birge, R. Eds.; Alan R. Liss: New York, 1986; p 159. (e) Wolber, P. K.; Hudson, B. S. *Biophys. J.* **1982**, *37*, 253. (f) Das, T. K.; Mazumdar, S. *Biophys. Chem.* **2000**, *86*, 15. (g) Sinha, S. S.; Mitra, R. K.; Pal, S. K. *J. Phys. Chem. B* **2008**, *112*, 4884.

(7) A preliminary study reveals complex time-dependent anisotropy profiles for some probe molecules in human serum albumin as well. These results will be published at a later stage.

(8) (a) Paul, A.; Samanta, A. *J. Phys. Chem. B* **2007**, *111*, 4724. (b) Mandal, P. K.; Samanta, A. *J. Phys. Chem. B* **2005**, *109*, 15172. (c) Karmakar, R.; Samanta, A. *J. Phys. Chem. A* **2003**, *107*, 7340. (d) Biswas, R.; Rohman, N.; Pradhan, T.; Buchner, R. *J. Phys. Chem. B* **2008**, *112*, 9379. (e) Rodriguez, J.; Marti, J.; Guardia, E.; Laria, D. *J. Phys. Chem. B* **2008**, *112*, 8990. (f) Seth, D.; Sarkar, S.; Sarkar, N. *Langmuir* **2008**, *24*, 7085. (g) Jin, H.; Li, X.; Maroncelli, M. *J. Phys. Chem. B* **2007**, *111*, 13473. (h) Sahu, K.; Mondal, S. K.; Ghosh, S.; Roy, D.; Sen, P.; Bhattacharyya, K. *J. Phys. Chem. B* **2006**, *110*, 1056.

(9) (a) Kunjappu, J. T. *J. Photochem. Photobiol. A: Chem.* **1993**, *71*, 269. (b) Chakraborty, A.; Seth, D.; Setua, P.; Sarkar, N. *J. Chem. Phys.* **2008**, *128*, 204510. (c) Mandal, U.; Ghosh, S.; Dey, S.; Adhikari, A.; Bhattacharyya, K. *J. Chem. Phys.* **2008**, *128*, 164505. (d) Ghosh, S.; Mondal, S. K.; Sahu, K.; Bhattacharyya, K. *J. Chem. Phys.* **2007**, *126*, 204708.

(10) (a) Chakraborty, A.; Seth, D.; Setua, P.; Sarkar, N. *J. Phys. Chem. B* **2006**, *110*, 16607. (b) Shobini, J.; Mishra, A. K.; Sandhya, K.; Chandra, N. *Spectrochim. Acta, Part A* **2001**, *57*, 1133.

(11) (a) Jones II, G.; Jackson, W. R.; Kanoktanaporn, S.; Halpern, A. M. *Opt. Commun.* **1980**, *33*, 315. (b) Jones II, G.; Jackson, W. R.; Choi, C.-Y. *J. Phys. Chem.* **1985**, *89*, 294. (c) Jones II, G.; Jackson, W. R.; Halpern, A. M. *Chem. Phys. Lett.* **1980**, *72*, 391. (d) Hicks, J. M.; Vandersall, M. T.; Babarogic, Z.; Eisenthal, K. B. *Chem. Phys. Lett.* **1985**, *116*, 18. (e) Hicks,

J. M.; Vandersall, M. T.; Sitzmann, E. V.; Eisenthal, K. B. *Chem. Phys. Lett.* **1987**, *135*, 413.

(12) Nag, A.; Bhattacharyya, K. *Chem. Phys. Lett.* **1990**, *169*, 12.

(13) (a) Longmuir, K. J.; Martin, O. C.; Pagano, R. E. *Chem. Phys. Lipids* **1985**, *36*, 197. (b) Schmidt, N.; Gercken, G. *Chem. Phys. Lipids* **1985**, *38*, 309. (c) Silvius, J. R.; Leventis, R.; Brown, P. M.; Zuckermann, M. *Biochemistry* **1987**, *26*, 4279. (d) Chattopadhyay, A. *Chem. Phys. Lipids* **1990**, *53*, 1. (e) Chattopadhyay, A.; London, E. *Biochim. Biophys. Acta* **1988**, *24*, 938.

(14) (a) Ghosh, P. B.; Whitehouse, M. W. *Biochem. J.* **1968**, *108*, 155. (b) Fager, R. S.; Kutina, C. B.; Abrahamson, E. W. *Anal. Biochem.* **1973**, *53*, 290. (c) Ferguson, S. J.; Lloyd, W. J.; Radda, G. K. *Biochem. J.* **1976**, *159*, 347.

(15) (a) Ramachandram, B.; Saha, S.; Samanta, A. *Chem. Phys. Lett.* **1998**, *290*, 9. (b) Ramachandram, B.; Samanta, A. *J. Phys. Chem. A* **1998**, *102*, 10579.

(16) Fery-Forgues, S.; Fayet, J. P.; Lopez, A. *J. Photochem. Photobiol. A: Chem.* **1993**, *70*, 229.

(17) Saha, S.; Samanta, A. *J. Phys. Chem. A* **1998**, *102*, 7903.

(18) Bonhote, P.; Dias, A. P.; Papageorgiou, N.; Kalyanasundaram, K.; Gratzel, M. *Inorg. Chem.* **1996**, *35*, 1168.

(19) López Arbeloa, T.; López Arbeloa, F.; Tapia José, M.; López Arbeloa, I. *J. Phys. Chem.* **1993**, *97*, 4704.

(20) Novo, M.; Soufi-Al, W. In *Fluorescence Study of the Supramolecular Interactions between Coumarins and Serum Albumins*; Proceedings of the International Electronic Conference on Synthetic Organic Chemistry; MDPI: Basel, Switzerland, 2007.

(21) Sali, A.; Blundell, T. L. *J. Mol. Biol.* **1993**, *234*, 779.

(22) Laskowski, R. A.; MacArthur, M. W.; Moss, D. S.; Thornton, J. M. *J. Appl. Crystallogr.* **1993**, *26*, 283.

(23) Lüthy, R.; Bowie, J. U.; Eisenberg, D. *Nature* **1992**, *356*, 83.

(24) Morris, G. M.; Goodsell, D. S.; Halliday, R. S.; Huey, R.; Hart, W. E.; Below, R. K.; Olson, A. J. *J. Comput. Chem.* **1998**, *19*, 1639.

(25) Mallick, A.; Haldar, B.; Chattopadhyay, N. *J. Phys. Chem. B* **2005**, *109*, 14683.

(26) Refer to Figure S1 of the Supporting Information provided.

(27) Ludescher, R. D.; Peting, L.; Hudson, S.; Hudson, B. *Biophysical Chemistry* **1987**, *28*, 59, and references therein.

(28) Peters, T. *Adv. Protein Chem.* **1985**, *37*, 161.

(29) Figure S2 of the Supporting Information shows 88% homology in the sequences of the BSA model and 1A06 (HSA).

(30) He, X. M.; Carter, D. C. *Nature* **1992**, *358*, 209.

(31) Sugio, S.; Kashima, A.; Mochizuki, S.; Noda, M.; Kobayashi, K. *Protein Eng.* **1999**, *12*, 439.

(32) Petitpas, I.; Bhattacharya, A. A.; Twine, S.; East, M.; Curry, S. *J. Biol. Chem.* **2001**, *276*, 22804.

(33) Dockal, M.; Chang, M.; Carter, D. C.; Rüker, F. *Protein Sci.* **2000**, *9*, 1455.

(34) Maes, V.; Engelborghs, Y.; Hoebeke, J.; Maras, Y.; Vercruysse, A. *Mol. Pharmacol.* **1982**, *21*, 100.

(35) Tian, J.; Liu, J.; He, W.; Hu, Z.; Yao, X.; Chen, X. *Biomacromolecules* **2004**, *5*, 1956.

(36) Zhang, Q.; Huang, Y.; Zhao, R.; Liu, G.; Chen, Y. *Biosens. Bioelectron.* **2008**, *24*, 48.

(37) Curry, S.; Brick, P.; Franks, N. P. *Biochim. Biophys. Acta* **1999**, *1441*, 131.

(38) Figure S3 of the Supporting Information shows the structural overlay of the BSA model and 1A06.

(39) Figure S4 of the Supporting Information provides the structural validation of BSA model.

(40) The docking energies of the molecules (in kcal/mol) obtained from AutoDock are−8.02 (C102),−8.25 (C153),−7.26 (C120),−7.04 (C152),−6.83 (C1),−7.70 (HNBD),−7.99 (MNBD),−8.24 (4NBD),−9.13 (6NBD), and−8.51 (7NBD).

(41) Ghuman, J.; Zunszain, P. A.; Petitpas, I.; Bhattacharya, A. A.; Otagiri, M.; Curry, S. *J. Mol. Biol.* **2005**, *353*, 38.

(42) Yuan, J. L.; Iv, Z.; Liu, Z. G.; Hu, Z.; Zou, G. L. *J. Photochem. Photobiol. A: Chem.* **2007**, *191*, 104.

(43) Tang, K.; Qin, Y. M.; Lin, A. H.; Hu, X.; Zou, G. L. *J. Pharm. Biomed. Anal.* **2005**, *39*, 404.

JP808611B